Morphological and biochemical analysis of the secretory pathway in melanoma cells with distinct metastatic potential

Inmaculada Ayala[a], Teresa Babià[a], Massimiliano Baldassarre[b], Arsenio Pompeo[b,c], Angels Fabra[d], Jan Willem Kok[e], Alberto Luini[b], Roberto Buccione[b], Gustavo Egea[a,*]

[a] *Dept. Biologica Cellular, Facultat de Medicina, Institut d'Investigacions Biomèdiques August Pi i Sunyer (IDIBAPS), Universitat de Barcelona, C/Casanova, 143, 08036 Barcelona, Spain*
[b] *Dept. of Cell Biology and Oncology, Istituto di Ricerche Farmacologiche Mario Negri, Consorzio Mario Negri Sud, 66030 S. Maria Imbaro (Chieti), Italy*
[c] *Dip.to Medicina Interna, Ospedale Floraspe Renzetti, 66034 Lanciano (Chieti), Italy*
[d] *Dept. Càncer i Metàstasi, Institut de Recerca Oncològica (IRO), Hospital Duran i Reynalds, 08907 Hospitalet de Llobregat, Barcelona, Spain*
[e] *Dept. Physiological Chemistry, University of Groningen 9713 AV, Groningen, The Netherlands*

Received 12 April 1999

Abstract In this report, we have investigated whether alterations of the morphological and functional aspects of the biosecretory membrane system are associated with the metastatic potential of tumor cells. To this end, we have analyzed the morphology of the Golgi complex, the cytoskeleton organization and membrane trafficking steps of the secretory pathway in two human melanoma A375 cell line variants with low (A375-P) and high metastatic (A375-MM) potential. Immunofluorescence analysis showed that in A375-P cells, the Golgi complex showed a collapsed morphology. Conversely, in A375-MM cells, the Golgi complex presented a reticular and extended morphology. At the ultrastructural level, the Golgi complex of A375-P cells was fragmented and cisternae were swollen. When the cytoskeleton was analyzed, the microtubular network appeared normal in both cell variants, whereas actin stress fibers were largely absent in A375-P, but not in A375-MM cells. In addition, the F-actin content in A375-P cells was significantly lower than in A375-MM cells. These morphological differences in A375-P cells were accompanied by acceleration and an increase in the endoplasmic reticulum to Golgi and the *trans*-Golgi network to cell surface membrane transport, respectively. Our results indicate that in human A375 melanoma cells, metastatic potential correlates with a well-structured morphofunctional organization of the Golgi complex and actin cytoskeleton.

Key words: Golgi complex; Actin; Secretory pathway; Metastasis; Cancer; A375

1. Introduction

All proteins destined for secretion, as well as those targeted to specialized organelles, undergo a series of conformational (secondary and tertiary structure acquisition) and chemical (glycosylation, sulfation, phosphorylation, etc.) post-translational modifications within the endoplasmic reticulum (ER) and the Golgi complex (GC). Furthermore, the GC itself is the most important protein sorting station in the cell [1]. In particular, it is at the *trans*-Golgi network (TGN), the most distal region of the GC, where proteins and lipids are sorted to their final destinations [2]. Thus, the GC plays a pivotal role in the cell physiology and has a highly conserved morphology in mammalian cells [3]. Some human diseases can be caused by defects in the intracellular protein and lipid traffic both in the secretory and endocytic pathways [4] and alterations in the GC can cause human disease or contribute to pathogenesis [5]. For example, morphological GC alterations such as fragmentation or hypertrophy have been described in certain viral diseases [6–8], in amyotrophic lateral sclerosis [9], in Alzheimer's disease [10,11] and in familial high density lipoprotein deficiency or Tangier disease [12]. Functional GC alterations have also been involved in cystic fibrosis [13], autosomal dominant polycystic kidney disease [14,15], type C Niemann-Pick disease [16], congenital sucrase-isomaltase disease [17] and in Lowe syndrome [18].

Fundamental features in human neoplasia are cell transformation and the acquisition of invasive and metastatic potential, one of the major causes of failure of many therapeutical approaches on the primary tumor. Alterations in the GC structure, abnormal distribution of Golgi markers in the ER and alterations in the intracellular traffic of proteins have been reported in cancer cells [19–22]. These disorders could contribute to the appearance of the aberrant glycosylation associated with cell transformation and metastasis [23–25]. Consequently, the study of the GC in tumor cells appears relevant since the majority of glycosyltransferases and glycohydrolases are compartmentalized in the GC [26].

To study the alterations of the biosecretory pathway associated with metastatic potential, we have used the human melanoma A375 cell line model. This cell model has been widely utilized in numerous invasion and metastasis studies ([27–30], amongst others). We report that the GC of A375-P cells is collapsed and fragmented, whereas in A375-MM cells, the GC displays a reticular and extended network. Furthermore, in A375-P cells, the morphological alterations in the GC are correlated with the disruption of the actin cytoskeleton and lead to an acceleration and an increased rate of the ER to Golgi and TG/TGN to cell surface transport routes, respectively. The significance of these results in relation with the metastatic potential is discussed.

2. Materials and methods

2.1. Cell culture

Human melanoma cell lines A375-P, A375-MM (characterized by low and high metastatic potential, respectively) were cultured in Dulbecco's modified Eagle's medium (DMEM) (Gibco BRL, Oxbridge,

*Corresponding author. Fax: (34) (93) 403 52 60.
E-mail: egea@medicina.ub.es

PII: S0014-5793(99)00620-1

UK) with Ham-F12 (1:1) supplemented with 10% fetal calf serum (FCS). The cells were grown at 37°C in a humidified atmosphere of 5% CO_2. Importantly, A375-P and A375-MM cell variants are periodically tested for their metastatic potential in vivo, according to their ability to form lung tumor nodules after i.v. injection [31].

2.2. Immunofluorescence

Cells were grown on coverslips to 70–90% confluence, washed in PBS (0.01 M phosphate buffer, 0.15 M NaCl, pH 7.2) and fixed either by immersion in cold methanol (−20°C) for 2 min or in freshly prepared paraformaldehyde (4% in PBS) at room temperature for 15 min. Cells were then washed in PBS and in the case of paraformaldehyde fixation, autofluorescence was quenched by incubation with 50 mM NH_4Cl in PBS for 30 min. Next, cells were permeabilized for 15 min with PBS containing 0.1% saponin and 1% BSA and processed for single or double staining immunofluorescence using the following primary antibodies: rabbit anti-mannosidase II (from Dr Velasco, University of Sevilla, Spain), rabbit anti-β-COP (from Dr T. Kreis, University of Geneva, Switzerland), TRITC-phalloidin (from a 0.2 mg/ml stock solution: Sigma, St. Louis, MO, USA). Polyclonal or monoclonal antibodies were visualized with TRITC or FITC anti-rabbit or anti-mouse IgG $(Fab')_2$ fragments (Boehringer Mannheim, Mannheim, Germany). Samples were viewed under an Olympus B×60 fluorescence microscope.

2.3. Transmission electron microscopy

Cells were washed twice in 0.1 M Na-cacodylate buffer (pH 7.4) and fixed with 2.5% glutaraldehyde in the same buffer for 30 min at room temperature. Cells were then washed three times for 5 min each with 0.1 M cacodylate buffer and post-fixed with 1% (v/v) OsO_4/1.5% (w/v) $K_4Fe(CN)_6$ in 0.1 M cacodylate buffer for 1 h at 4°C. Cells were scraped from the dishes and centrifuged. Cell pellets were rinsed in distilled water and stained en bloc with 1% aqueous uranyl acetate for 1 h, followed by dehydration through graded ethanol solutions and embedded in Epon 812. Ultrathin sections were stained with lead citrate for 2 min and observed with a Philips 301 electron microscope.

2.4. Fluorescent phalloidin binding assay (F-actin content)

Cell cultures were fixed in 4% paraformaldehyde in PBS for 15 min and permeabilized with 0.1% Triton X-100 in PBS for 5 min. After three washes in PBS, cells were incubated with TRITC-phalloidin (from a 0.2 mg/ml stock solution) in PBS for 15 min, washed three times in PBS and extracted with methanol for 25 min at room temperature. The fluorescence intensity of the supernatants was quantified in a Kontron Instruments fluorimeter (SFM25) at 554 nm and 573 nm excitation and emission wavelengths, respectively.

2.5. Virus infection and vesicular stomatitis virus (VSV)-G transport assay by the Endo H resistance form acquisition

Cell monolayers were infected with the ts045 temperature-sensitive mutant VSV in DMEM without serum at 32°C. At 4 h post-infection in DMEM containing 10% FCS, cells were incubated for 15 min in methionine-free DMEM at 40°C and pulse-labelled in suspension for 10 min with 100 μCi/ml Pro-Mix[^{35}S] (Amersham, Buckinghamshire, UK) at 40°C. Cells were washed with ice-cold PBS and chased at 32°C in methionine-containing media for the indicated times. Cells were then washed twice with ice-cold PBS and lysed for 15 min on ice with Triton X-100 lysis buffer (1% Triton X-100, 50 mM Tris-HCl, pH 8.0, 62.5 mM EDTA) at 4°C for 30 min and centrifuged at 14 000 rpm for 15 min. 200 μl of detergent solution (62.5 mM EDTA, 50 mM Tris-HCl, pH 8.0, 0.4% DOC, 1% NP40), 8.5 μl of 10% SDS and 2 μl of mouse monoclonal P5D4 anti-VSV-G protein antibody (Sigma, St. Louis, MO, USA) were added to supernatants overnight at 4°C. Next, rabbit anti-mouse IgG (DAKO, Denmark) was added for 1 h at room temperature and 20 μl of protein A/G agarose (Santa Cruz Biotechnology, Santa Cruz, CA, USA) was added for 45 min at room temperature. The pellet was washed three times in RIPA buffer (10 mM Tris-HCl pH 7.4, 0.1% SDS, 1% DOC, 1% NP40, 0.15 M NaCl), three times in TENEN high salt buffer (10 mM Tris-HCl, pH 7.2, 0.5 M NaCl, 1 mM EDTA, 0.5% NP40, 0.1% SDS) and twice in PBS. Protein A/G agarose beads were resuspended in 10 μl BH1 buffer (0.1 M sodium acetate, pH 5.5, 1% SDS, 0.1% Triton X-100) and proteins were eluted from the beads by heating at 95°C for 5 min. The supernatant was recovered by centrifugation and 30 μl BH2 buffer (0.1 M sodium acetate, pH 5.5, 1 mM PMSF, 5 μg/ml aprotinin, 1 mM benzamidin) was added. To assay the Endo H-sensitivity, 0.25 mU Endo H (Boehringer Mannheim, Mannheim, Germany) was added and the reaction was performed overnight at 37°C. Samples were analyzed under reducing conditions in 7.5% SDS-PAGE and gels were fluorographed. Band quantitation was performed with the

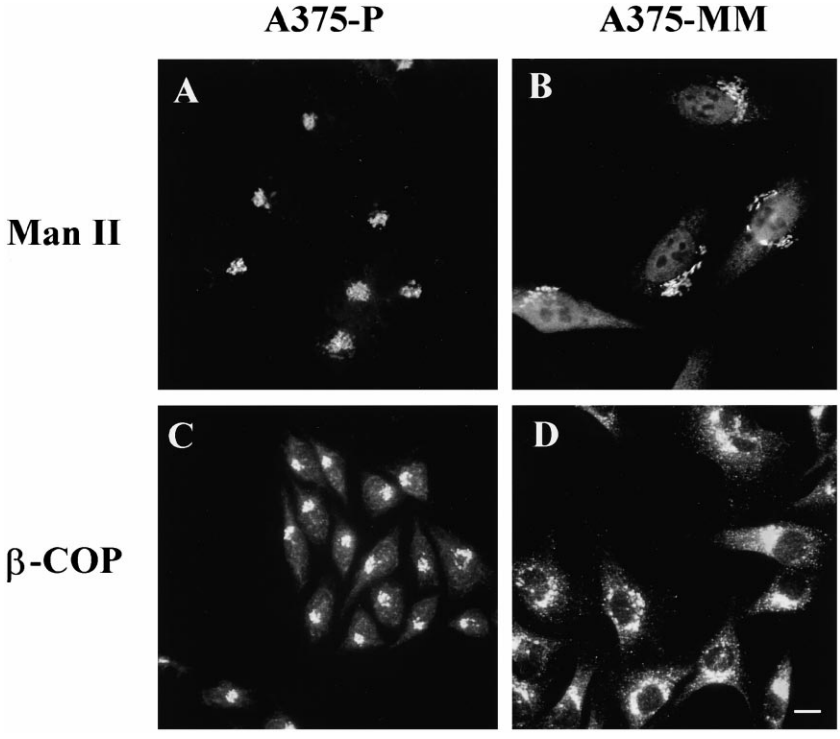

Fig. 1. Immunofluorescence microscopy showing the morphology of the GC stained for the Golgi resident protein mannosidase II (ManII) (A, B) and the Golgi-associated protein β-COP (C, D) in A375-P (A, C) and A375-MM (B, D) cells. In A375-P cells, the GC is collapsed in a juxta- or supranuclear positioning, whereas in A375-MM cells, the GC shows a reticular and extended morphology with perinuclear localization.

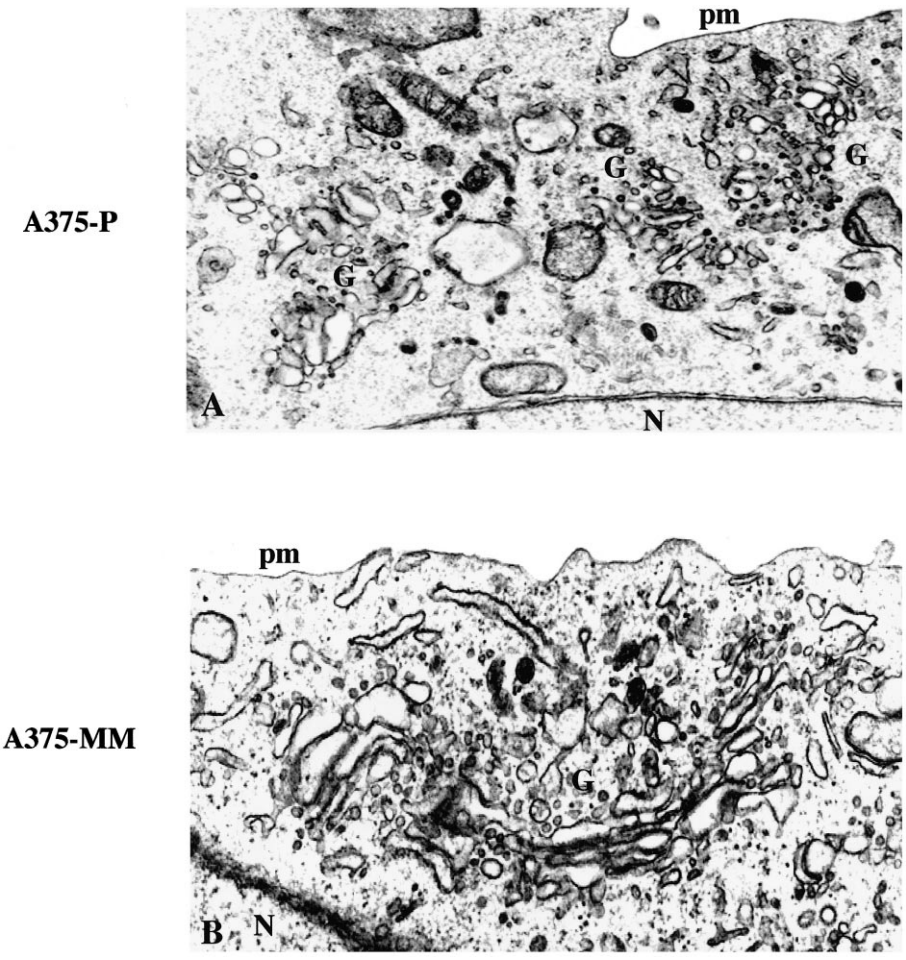

Fig. 2. Transmission electron microscopy of the GC in A375-P and A375-MM cells. In A375-P cells (A), the GC shows a disorganized structure with cisternal fragmentation and swelling. Conversely, the GC of the A375-MM cells (B) presents the common stacked morphology of flattened cisternae. GC, Golgi complex; N, nucleus.

Phoretix image analysis software (Phoretix International, Newcastle, UK).

2.6. Constitutive release of glycosaminoglycans (GAGs)

Cells cultured at confluence in 12 well plates were washed, incubated with xyloside for 15 min, labelled with [^{35}S]sulfate and treated for release as described previously [32]. Release media were collected and centrifuged ($14\,000\times g$, 5 min) and the supernatants recovered. Cell monolayers were extracted with 0.5 ml of 0.1 M NaOH for at least 30 min at 37°C. [^{35}S]sulfate-labelled GAGs were quantified by a precipitation assay. Briefly, cell supernatants and extracts (0.5 ml) were precipitated overnight at room temperature by the addition of chondroitin sulfate (0.5 mg/ml final concentration) and cetylpyridinium chloride (1% final concentration). Precipitates were recovered by centrifugation ($4000\times g$ for 10 min) and washed twice with 1% cetylpyridinium chloride in NaCl (20 mM). Finally, pellets were dissolved in NaCl (2 M) at 37°C and the radioactivity was measured in a scintillation counter.

3. Results

The morphology of the GC was studied at the immunofluorescence level with antibodies against the *cis*/middle Golgi marker mannosidase II (Figs. 1A, B and 3B, D). In A375-P cells, the GC appeared with a collapsed morphology in a juxta- or supranuclear position (Figs. 1A and 3B) while in A375-MM cells, the GC showed a reticular and extended morphology and was perinuclearly located (Fig. 1B and 3D). Similar results were obtained when both cell variants were immunostained for the Golgi-associated protein β-COP (Fig. 1C, D) and for other Golgi resident protein markers such as MG-160 or galactosyltransferase (not shown). When the Golgi ultrastructure was studied at the EM level in A375-P cells, the GC was fragmented with shortened and swollen cisternae (Fig. 2A). On the contrary, A375-MM cells featured a GC with long and flattened cisternae (Fig. 2B).

It is well known that the GC morphology and subcellular positioning is determined by the cytoskeleton organization [33]. We thus studied the microtubule and actin cytoskeletons in both cell variants. Immunofluorescence staining of microtubules with anti-β-tubulin antibodies showed that the microtubular cytoskeleton was not altered either in A375-P and A375-MM cells (not shown). On the other hand, it has recently been shown that the GC morphology is also maintained by actin microfilaments [22,34]. Therefore, A375 cell variants were double-stained for GC with anti-mannosidase II antibodies and for polymerized actin with phalloidin (Fig. 3). A375-P cells presented fewer actin stress fibers than A375-MM cells (Fig. 3A and C, respectively). This morphological difference in the arrangement of actin was confirmed by the F-actin quantitation. Indeed, in A375-P cells, the F-actin content was significantly lower than in A375-MM cells (Fig. 3E).

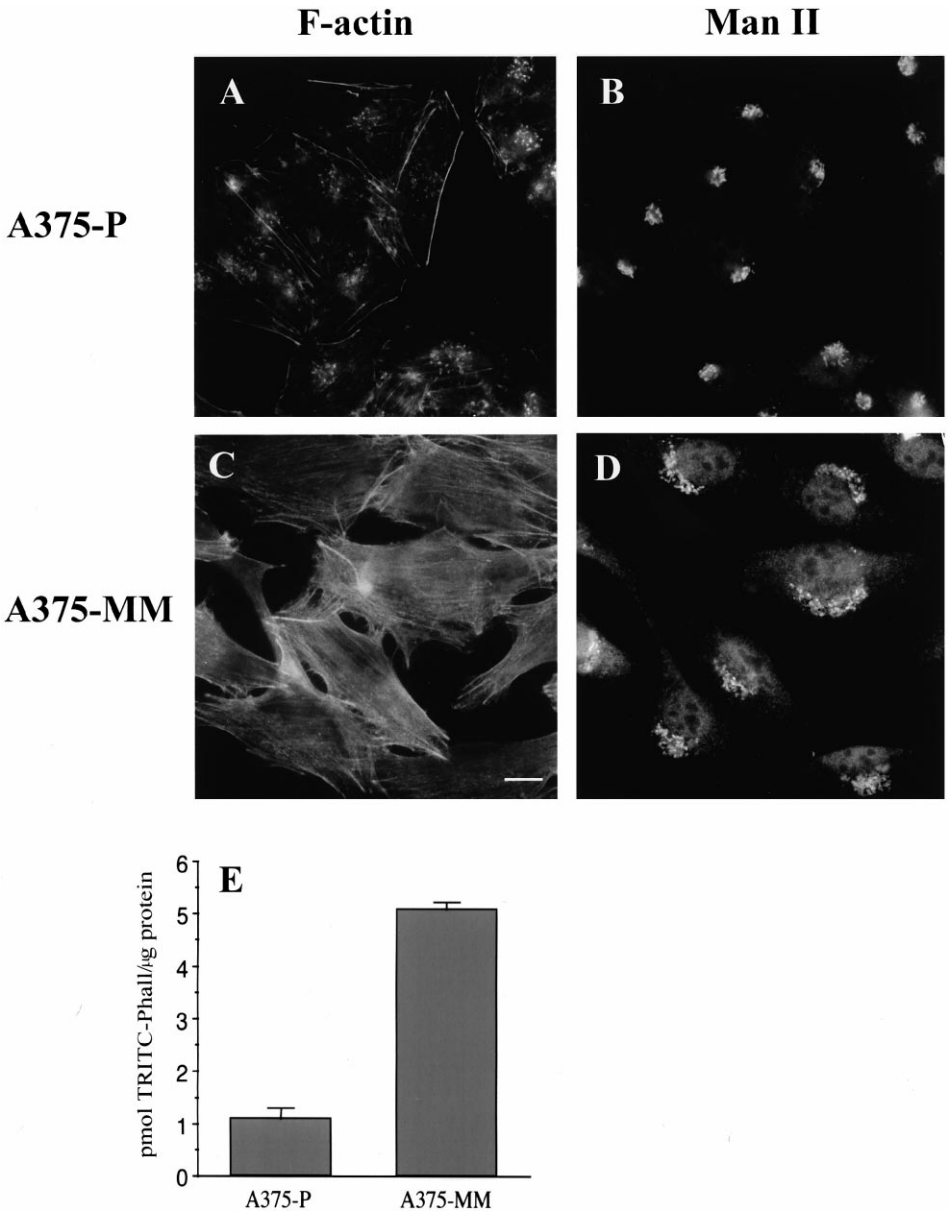

Fig. 3. Fluorescence double staining of F-actin (A, C) and the GC (B, D) and quantitative analysis of the F-actin content (E) in A375-P (A, B) and A375-MM (C, D) cells. Phalloidin staining of polymerized actin clearly shows that A375-P cells contain less actin stress fibers than A375-MM cells. This visual observation is quantitatively confirmed when the F-actin content is measured (E). Note the different GC morphology in both cell variants already shown in Fig. 1.

To assess the physiological significance of the differences in GC morphology between the A375 cell variants, we investigated whether there were alterations in membrane transport along the secretory pathway. In particular, we have analyzed biochemically the ER to GC and the TG/TGN to cell surface transport steps. The ER to GC transport was assayed by studying differences in the processing of newly synthesized VSV-G glycoprotein to the Endo H resistant form. In A375-P cells, a more rapid acquisition of VSV-G Endo H resistance was observed, relative to A375-MM cells (Fig. 4). Subsequently, we have studied the constitutive TG/TGN to cell surface membrane transport step. Thus, [^{35}S]sulfate-labelled GAGs were used as markers [32,35] because GAGs are soluble and are sulfated at the most distal Golgi compartments [36,37]. As can be observed in Fig. 5, the time course of constitutive GAGs release indicates that their transport is significantly higher in A375-P versus A375-MM cells.

4. Discussion

We have investigated the structural and functional alterations of the secretory pathway associated with the metastatic potential in a well-established human metastatic melanoma model, the A375 cell line. To our knowledge, this is the first study that attempts to associate alterations of the constitutive secretory pathway with metastatic potential. Initially, we focused on the GC since this organelle is the central processing and sorting station of the secretory pathway. At the immunofluorescence level, the GC of A375-MM cells showed a reticular and extended morphological network with a perinuclear

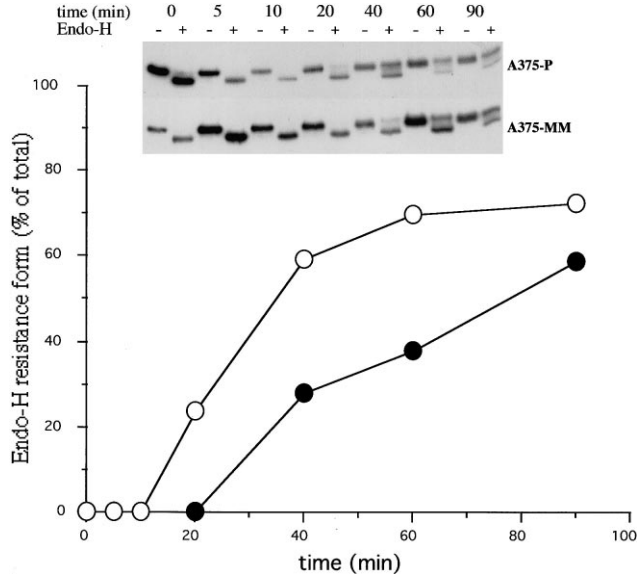

Fig. 4. ER to Golgi transport of the VSV-G glycoprotein in A375-P and A375-MM cells. Note that in A375-P cells (○), VSV-G acquires the Endo H resistant form faster than in A375-MM cells (●). Strikingly, in both cell variants, the complete acquisition of the Endo H resistant form is not completed even at very long times of chase. A representative experiment is shown in the inset.

location, but in A375-P cells, the GC appeared collapsed in a supra- or juxtanuclear area. Ultrastructurally, in A375-P cells, the Golgi stacks were fragmented and presented swelling of cisternae. These morphological alterations resemble those observed in NRK cells when treated with actin-disrupting agents such as cytochalasin D [24] or conditionally transformed by oncogenic N-*ras* [22]. We thus analyzed the state of the actin cytoskeleton in both A375 cell line variants. In A375-P cells, actin stress fibers were poorly organized relative to the abundant and well-organized ones of the A375-MM cells. These morphological differences were confirmed by the biochemical measurement of the F-actin content. Thus, our results indicate that the lower metastatic potential of A375-P cells is associated with a collapsed GC morphology, a low F-actin content and a reduced presence of actin stress fibers. Similar results

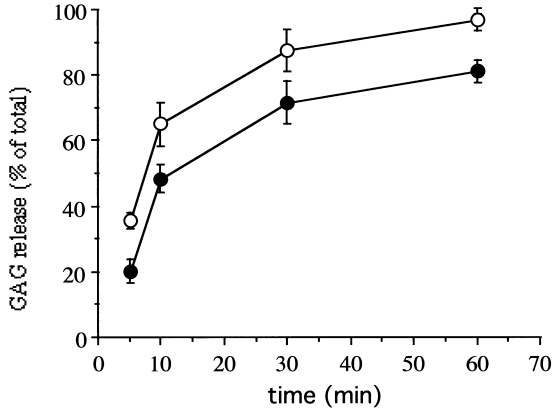

Fig. 5. Constitutive glycan transport from the TG/TGN to the cell surface in A375-P and A375-MM cells. Note that in A375-P cells (○), the rate of GAG release is significantly higher than in A375-MM cells (●). Values represent means ± S.D. from three independent experiments.

were also observed in another human melanoma cell line with a low metastatic potential (A2058: I. Ayala, A. Fabra and G. Egea, unpublished observations). Our results are in accordance with those indicating that the ability of tumor cells to invade and metastasize is correlated to increased levels of polymerized actin, which itself depends on Rho-mediated signal transduction pathways [38–40]. Interestingly, drugs that alter actin polymerization have been shown to reduce tumor growth and the metastatic potential [38,41–43]. Previously, we have demonstrated that the GC morphology is associated with actin microfilaments [22,34]. The current study indicates that, in the human melanoma A375 cell line, metastatic potential is correlated with a well-structured GC and actin cytoskeleton. On the contrary, low metastatic potential is characterized by actin disassembly, a low F-actin content and, consequently, the morphological collapse of the GC. Interestingly, in undifferentiated human colon carcinoma HT29 cells, it has been reported that the GC was exclusively associated with actin microfilaments and Golgi cisternae were also swollen [44]. Furthermore, the disappearance or absence of actin stress fibers and decreasing F-actin content levels have been reported to be correlated with cell transformation [45,46].

Finally, we have also observed that A375-P cells show a shorter doubling time than A375-MM cells (I. Ayala, G. Egea and A. Fabra, unpublished results). It is tempting to speculate that the morphofunctional alterations of the GC are a consequence of this higher proliferative activity. Thus, cells with a higher proliferative activity would not require a well-structured GC. This could also be a consequence of having a poorer actin cytoskeleton organization. Furthermore, as a consequence of the higher proliferation rate, A375-P cells could feature higher and/or accelerated ER to Golgi and TGN to cell surface transport rates because of the increased requirement for membrane components. On the contrary, in A375-MM cells, the proliferative rate is not so high and thus, there is a better organized actin cytoskeleton and structured GC.

Acknowledgements: We thank Maite Muñoz for the technical support, Dr E. Berger, Dr N. Gonatas, Dr A. Velasco and the late Dr T. Kreis for generous providing of antibodies. I.A. is the recipient of a predoctoral fellowship from the Ministerio de Educación y Cienca, Spain. This work was supported by Grants to G.E. (CICYT SAF 97/0016 and TeleMarató de Catalunya TV3), to A.F. (CICYT SAF 98/0049) and to A.L. (Italian National Research Council, Progretto Finalizzato 'Biotecnologie' Contract n. 970130549 and Italian Association for Cancer Research, AIRC). Support by the Italian Foundation for Cancer Research (FIRC) to A.L. and R.B. is also acknowledged.

References

[1] Farquhar, M.G. and Hauri, H.P. (1997) In: The Golgi Apparatus (Berger, E.G. and Roth, J., Eds.) pp. 63–130, Birkhäuser, Basel.
[2] Keller, P. and Simons, K. (1997) J. Cell Sci. 110, 3001–3009.
[3] Rambourg, A. and Clermont, Y. (1997) in: The Golgi Apparatus (Berger, E.G. and Roth, J., Eds.) pp. 37–62, Birkhäuser, Basel.
[4] Amara, J.F., Cheng, S.H. and Smith, A.E. (1992) Trends Cell Biol. 2, 145–148.
[5] Gonatas, N.K. (1997) In: The Golgi Apparatus (Berger, E.G. and Roth, J., Eds.) pp. 247–273, Birkhäuser, Basel.
[6] Campadelli, G., Brandimarti, R., Di Lazzaro, C., Ward, P.L., Roizman, G. and Torrisi, M.R. (1993) Proc. Natl. Acad. Sci. USA 90, 2798–2802.
[7] Lavi, E., Wang, Q., Weiss, S.R. and Gonatas, N.K. (1992) Virology 221, 325–334.

[8] Sandoval, I.V. and Carrasco, L. (1997) J. Virol. 71, 4679–4693.
[9] Mourelatos, Z., Adler, H., Hirano, A., Donnenfeld, H., Gonatas, J.O. and Gonatas, N.K. (1990) Proc. Natl. Acad. Sci. USA 87, 4393–4395.
[10] Salehi, A., Ravid, R., Gonatas, N.K. and Swaab, D.E. (1995) J. Neuropathol. Exp. Neurol. 54, 704–709.
[11] Stieber, A., Mourelatos, Z. and Gonatas, N.K. (1996) Am. J. Pathol. 148, 415–426.
[12] Robenek, H. and Schmitz, G. (1991) Arterioscler. Thromb. 11, 1007–1020.
[13] Barasch, J. and Al-Awqati, Q. (1992) Trends Cell Biol. 2, 35–37.
[14] Liu, Z.Z., Carone, F.A., Nakamura, S. and Kanwar, Y.S. (1992) Am. J. Physiol. 263, F697–F704.
[15] Carone, F.A., Jin, H., Nakamura, S. and Kanwar, Y.S. (1993) Lab. Invest. 68, 413–418.
[16] Blanchette-Mackie, E.J., Dwyer, N.K., Amende, L.M., Kruth, H.S., Butler, J.D., Sokol, J., Comly, M.E., Vanier, M.T., August, J.T., Brady, R.O. and Pentchev, P.G. (1988) Proc. Natl. Acad. Sci. USA 85, 8022–8026.
[17] Hauri, H.-P., Roth, J., Sterchi, E.E. and Lentze, M.J. (1985) Proc. Natl. Acad. Sci. USA 82, 4434.
[18] Suchy, S.F., Olivos-Glander, I.M. and Nussbaum, R.L. (1995) Hum. Mol. Genet. 4, 2245–2250.
[19] Seguchi, T., Goto, Y., Ono, M., Fujiwara, T., Shimada, T., Kung, H.-J., Nishioka, M., Ikehara, Y. and Kuwano, M. (1992) J. Biol. Chem. 267, 11626–11630.
[20] Egea, G., Francí, C., Gambus, G., Lesufleur, T., Zweibaum, A. and Real, F.X. (1993) J. Cell Sci. 105, 819–830.
[21] Francí, C., Egea, G., Arribas, M., Reuser, J.J.A. and Real, F.X. (1996) Biochem. J. 314, 33–40.
[22] Babià, T., Ayala, I., Valderrama, F., Mato, E., Bosch, M., Santarén, J.F., Renau-Piqueras, J., Kok, J.W., Thomson, T.M. and Egea, G. (1999) J. Cell Sci. 112, 477–489.
[23] Hakomori, S.I. (1989) Adv. Cancer Res. 52, 257–331.
[24] Saitoh, O., Wang, W.-C., Lotan, R. and Fukuda, M. (1992) J. Biol. Chem. 267, 5700–5711.
[25] Dennis, J.W. (1992) in: Cell Surface Carbohydrates and Cell Development (Fukuda, M., Ed.) pp. 161–194, CRC Press, Boca Ratón.
[26] Roth, J. (1997) In: The Golgi apparatus. Edited by Berger E.G., Roth J. Basel, Birkhäuser, pp. 131–161.
[27] Welch, D.R., Bisi, J.E., Miller, B.E., Conaway, D., Seftor, E.A., Yohem, K.H., Gilmore, L.B., Seftor, R.E., Nakajima, M. and Hendrix, M.J. (1991) Int. J. Cancer 47, 227–237.
[28] Gehlsen, K.R., Davis, G.E. and Sriramarao, P. (1992) Clin. Exp. Metastasis 10, 111–120.
[29] Yeatman, T.J., Updyke, T.V., Kaeztel, M.A., Dedman, J.R. and Nicolson, G.L. (1993) Clin. Exp. Metastasis 11, 37–44.
[30] Singh, R.K., Gutman, M. and Radinsky, R. (1995) J. Interf. Cytokine Res. 15, 81–87.
[31] Kozlowski, J.M., Hart, I.R., Fidler, I.J. and Hanna, N. (1984) J. Natl. Cancer Inst. 72, 913–917.
[32] Buccione, R., Bannykh, S., Santone, I., Baldassarre, M., Facchiano, F., Bozzi, Y., Di Tullio, G., Mironov, A., Luini, A. and De Matteis, M.A. (1996) J. Biol. Chem. 271, 3523–3533.
[33] Kreis, T.E., Goodson, H.V., Perez, F. and Rönnholm, R. (1997) in: The Golgi Apparatus (Berger, E.G. and Roth, J., Eds.) pp. 179–194, Birkhäuser, Basel.
[34] Valderrama, F., Babià, T., Ayala, I., Kok, J.W., Renau-Piqueras, J. and Egea, G. (1998) Eur. J. Cell Biol. 76, 9–17.
[35] Brion, C., Miller, S.G. and Moore, H.-P.H. (1992) J. Biol. Chem. 267, 1477–1483.
[36] Baeuerle, P.A. and Huttner, W.B. (1987) J. Cell. Biol. 105, 2655–2664.
[37] Graham, J.M. and Winterbourne, D.J. (1988) Biochem. J. 252, 437–445.
[38] Verschueren, H., De Baetselier, P., De Braekeleer, J., Dewit, J., Aktories, K. and Just, I. (1997) Eur. J. Cell Biol. 73, 182–187.
[39] Verschueren, H., van der Taelen, I., Dewit, J., De Brakeleer, J., De Baetselier, P., Aktories, K. and Just, I. (1995) Eur. J. Cell Biol. 66, 335–341.
[40] Yoshioka, K., Matsumura, F., Akedo, H. and Itoh, K. (1998) J. Biol. Chem. 273, 5146–5154.
[41] Bousquet, P.F., Paulsen, L.A., Fondy, C., Lipski, M., Loucy, K.J. and Fondy, T.P. (1990) Cancer Res. 50, 1431–1439.
[42] Stournaras, C., Stiakaki, E., Koukouritaki, S.B., Theodoropoulos, P.A., Kalmanti, M., Fostinis, Y. and Gravanis, A. (1996) Biochem. Pharmacol. 52, 1339–1346.
[43] Jordan, M.A. and Wilson, L. (1998) Curr. Opin. Cell. Biol. 10, 123–130.
[44] Chazaud, B., Muriel, M.-P., Aubery, M. and Decastel, M. (1996) Differentiation 60, 179–191.
[45] Rao, J.Y., Hemstreet, G.P., Hurst, R.E., Bonner, R.B., Min, K.W. and Jones, P.L. (1990) Cancer Res. 50, 2215–2220.
[46] Rao, K.M. and Cohen, H.J. (1990) Mutat. Res. 256, 139–148.